Supporting Information

One-pot synthesis of azabora[6]helicence by a Schiff base forming reaction

Yuto Kage,[a] Yuchuan Jiang,[a] Namiki Minakuchi,[a] Shigeki Mori[b] and Soji Shimizu*[a]

[a]Department of Applied Chemistry, Graduate School of Engineering and Centre for Molecular Systems, Kyushu University, Fukuoka 819-0395, Japan

[b]Advanced Research Support Centre (ADRES), Ehime University, Matsuyama 790-8577, Japan

Contents:

i. Experimental

General procedure: High-resolution mass spectrometry was performed on a JEOL LMS-HX-110 spectrometer (FAB mode with 3-nitrobenzyl alcohol (NBA) as a matrix). ^{1}H NMR spectra were recorded on a JEOL JNM-ECX500R spectrometer (operating at 495.132 MHz for ^{1}H and 465.8894 MHz for ^{19}F) using residual solvent as an internal reference for ^{1}H (δ = 7.26 ppm for $CDCl_3$) and using trifluoroacetic acid as an external reference for ^{19}F (δ = –76.55 ppm). Electronic absorption spectra were recorded on a JASCO V-770 spectrophotometer. Fluorescence spectra in solution were measured on an SPEX Fluorolog-3-NIR spectrometer (HORIBA) with a NIR-PMT R5509 photomultiplier tube (Hamamatsu) or an on a JASCO FR-8650 spectrometer. Fluorescence spectra in a drop-cast film and absolute fluorescence quantum yields in solution and a drop-cast film were measured on a HAMAMATSU C13534-21 calibrated integrating-sphere system with and without self-absorption correction for solution samples and film samples, respectively. Preparative separations were performed using silica gel column chromatography (KANTO Silica Gel 60 N, spherical, neutral, 40–50 μm or KANTO Silica Gel 60 N, spherical, neutral, 63–210 μm). Thin-layer chromatography (TLC) was performed with aluminum sheet silica gel 60 F_{254} (Merck). All reagents and solvents used for syntheses were of commercial reagent grade and were used without further purification except where noted. Spectroscopic grade solvents were used for spectroscopy.

Crystallographic data collection and structure refinement: Suitable crystals for X-ray diffraction analysis were obtained by a vapor diffusion method. Data collection was carried out at –173 °C on a Rigaku Saturn724 diffractometer with MoKα radiation. The structure was solved by a direct method (SHELXT)[1] and refined using a full-matrix least squares technique (SHELXL).[2] CCDC 2320994 and 2320995 contain the supplementary crystallographic data for this paper. These data can be obtained free of charge via www.ccdc.cam.ac.uk/data_request/cif, or by emailing data_request@ccdc.cam.ac.uk, or by contacting The Cambridge Crystallographic Data Centre, 12 Union Road, Cambridge CB2 1EZ, UK; fax: +44 1223 336033.

Electrochemical measurements: Cyclic voltammograms (CV) and differential pulse voltammograms (DPV) were recorded on a CH Instrument Model 620B (ALS) under an argon atmosphere in an *o*-dichlorobenzene (*o*-DCB) solution with 0.1 M tetra-*n*-butylammonium perchlorate (TBAP) as a supporting electrolyte. Measurements were made with a glassy carbon working electrode, a Ag/AgCl reference electrode and a Pt wire counter electrode. The concentration of the solution was fixed at 0.5 mM, and the scan rates were set to 100 mV s^{-1} for CV measurements. The pulse amplitude and width were set to 0.05 V and 0.2 s for DPV measurements. A ferrocenium/ferrocene (Fc^{+}/Fc) couple was used as an internal standard.

Theoretical calculation details: The Gaussian 16 software package[3] was used to perform DFT and TDDFT calculations using the B3LYP[4] with 6-311G(2d,p) basis set.[5]

Synthetic procedure

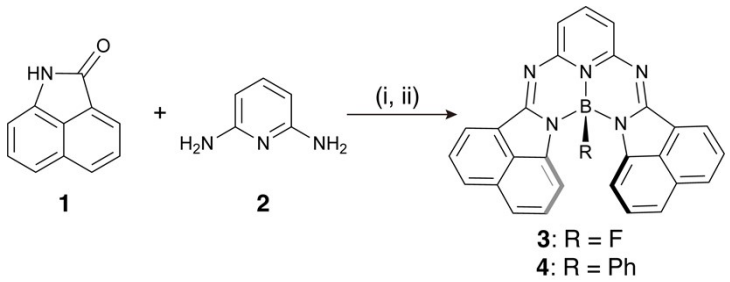

Scheme S1. Synthesis of azabora[6]helicenes **3** and **4**. Reaction conditions (i): $TiCl_4$, NEt_3, toluene, reflux; (ii) $BF_3{\cdot}OEt_2$ for **3** and (i) $TiCl_4$, NEt_3, *o*-dichlorobenzene, reflux; (ii) $BPh_3{\cdot}PPh_3$ and NEt_3 for **4**.

3: Benzo[*cd*]indol-2-(1H)-one **1** (504 mg, 2.98 mmol, 2.8 eq) and 2,6-diaminopyridine **2** (115 mg, 1.05 mmol) were dissolved in dry toluene (93 mL). The mixture was stirred at 25 °C for 10 min under a nitrogen atmosphere before adding titanium tetrachloride (144 μL, 1.31 mmol, 1.3 eq) and triethylamine (456 μL, 3.29 mmol). The reaction mixture was then refluxed overnight. Boron trifluoride etherate (768 μL, 6.22 mmol, 5.9 eq) was added, and the mixture was refluxed for 3 h. The resulting mixture was directly charged to silica gel chromatography. The roughly purified mixture was further purified by silica gel column chromatography (eluent: EtOAc/hexane = 1:1 (v/v)) to provide **3** as a black solid (84.0 mg, 191 μmol, 18%).

^{1}H NMR (495 MHz, $CDCl_3$, 295 K): δ 8.42–8.38 (m, 2H), 8.18 (d, J = 7.9 Hz, 1H), 8.12 (d, J = 7.9 Hz, 1H), 8.01 (t, J = 7.9 Hz, 1H), 7.88–7.82 (m, 2H), 7.73 (d, J = 8.5 Hz, 1H), 7.64–7.60 (m, 2H), 7.45 (d, J = 7.9 Hz, 1H), 7.39 (dd, J_1 = J_2 = 7.7 Hz, 1H), 7.35 (d, J = 7.9 Hz, 1H), 6.87 (d, J = 6.8 Hz, 1H), 6.41 (d, J = 7.4 Hz, 1H). ^{1}H NMR (495 MHz, tetrachloroethane-d_2, 295 K): δ 8.71 (s, 1H), 8.52 (d, J = 6.8 Hz, 1H), 8.26 (m, 2H), 8.12 (t, J = 7.9 Hz, 1H), 7.93 (m, 2H), 7.83 (d, J = 8.5 Hz, 1H), 7.75 (d, J = 7.9 Hz, 2H), 7.68 (dd, J_1 = J_2 = 7.7 Hz, 1H), 7.52 (d, J = 7.9 Hz, 1H), 7.47 (dd, J_1 = J_2 = 7.9 Hz, 1H), 6.97 (d, J = 6.8 Hz, 1H), 6.56 (d, J = 7.4 Hz, 1H). ^{19}F NMR (465 MHz, $CDCl_3$, 295 K): δ –129.710 (q, J_{B-F} = 51.2 Hz). UV/Vis/NIR ($CHCl_3$): λ_{max} [nm] (ε [$M^{-1}cm^{-1}$]) = 358 (10400), 415 (27800), 437 (20300), 513 (18200), 548 (19000); HR-MS (FAB): [M]$^+$ Calcd for $C_{27}H_{15}BFN_5$: 439.1409; Found: 439.1404 (error: –1.1 ppm).

4: Benzo[*cd*]indol-2-(1H)-one **1** (253 mg, 1.50 mmol, 2.8 eq) and 2,6-diaminopyridine **2** (54.5 mg, 0.50 mmol) were dissolved in dry *o*-dichlorobenzene (25 mL). The mixture was stirred at 25 °C for 10 min under a nitrogen atmosphere before adding titanium tetrachloride (43.8 μL, 0.40 mmol, 2.0 eq) and triethylamine (200 μL, 1.43 mmol). The reaction mixture was then refluxed for 2 h. Triphenylborane-triphenylphosphine complex (131 mg, 0.26 mmol, 1.3 eq) and triethylamine (200 μL, 1.43 mmol) were added, and the mixture was refluxed for 3 h. The resulting mixture was directly charged to silica gel chromatography. The roughly purified mixture was further purified by silica gel column chromatography (eluent: EtOAc/hexane = 1:1 (v/v)) to provide **4** as a red solid (31.8 mg, 64 μmol, 13%).

^{1}H NMR (495 MHz, $CDCl_3$, 295 K): δ 8.38 (m, 2H), 8.15 (d, J = 7.9 Hz, 1H), 8.09 (d, J = 7.9 Hz, 1H), 7.91 (t, J = 7.9 Hz, 1H), 7.84 (m, 2H), 7.61 (d, J = 7.9 Hz, 1H), 7.56 (d, J = 8.5 Hz, 1H), 7.38–7.32 (m, 3H), 7.19 (d, J = 7.4 Hz, 1H), 6.95 (t, J = 7.1 Hz, 1H), 6.89 (dd, J_1 = 7.1 Hz, J_2 = 6.8 Hz, 2H), 6.77 (d, J = 6.8 Hz, 2H), 6.42 (d, J = 6.8 Hz, 1H), 6.35 (d, J = 7.4 Hz, 1H). UV/Vis/NIR ($CHCl_3$): λ_{max} [nm] (ε [$M^{-1}cm^{-1}$]) = 360 (7700), 417 (22000), 442 (28000), 518 (14800), 554 (16000); HR-MS (FAB): [M]$^+$ Calcd for $C_{33}H_{21}BN_5$: 498.1896; Found: 498.1892 (error: –0.8 ppm).

ii. HR-MS Spectra

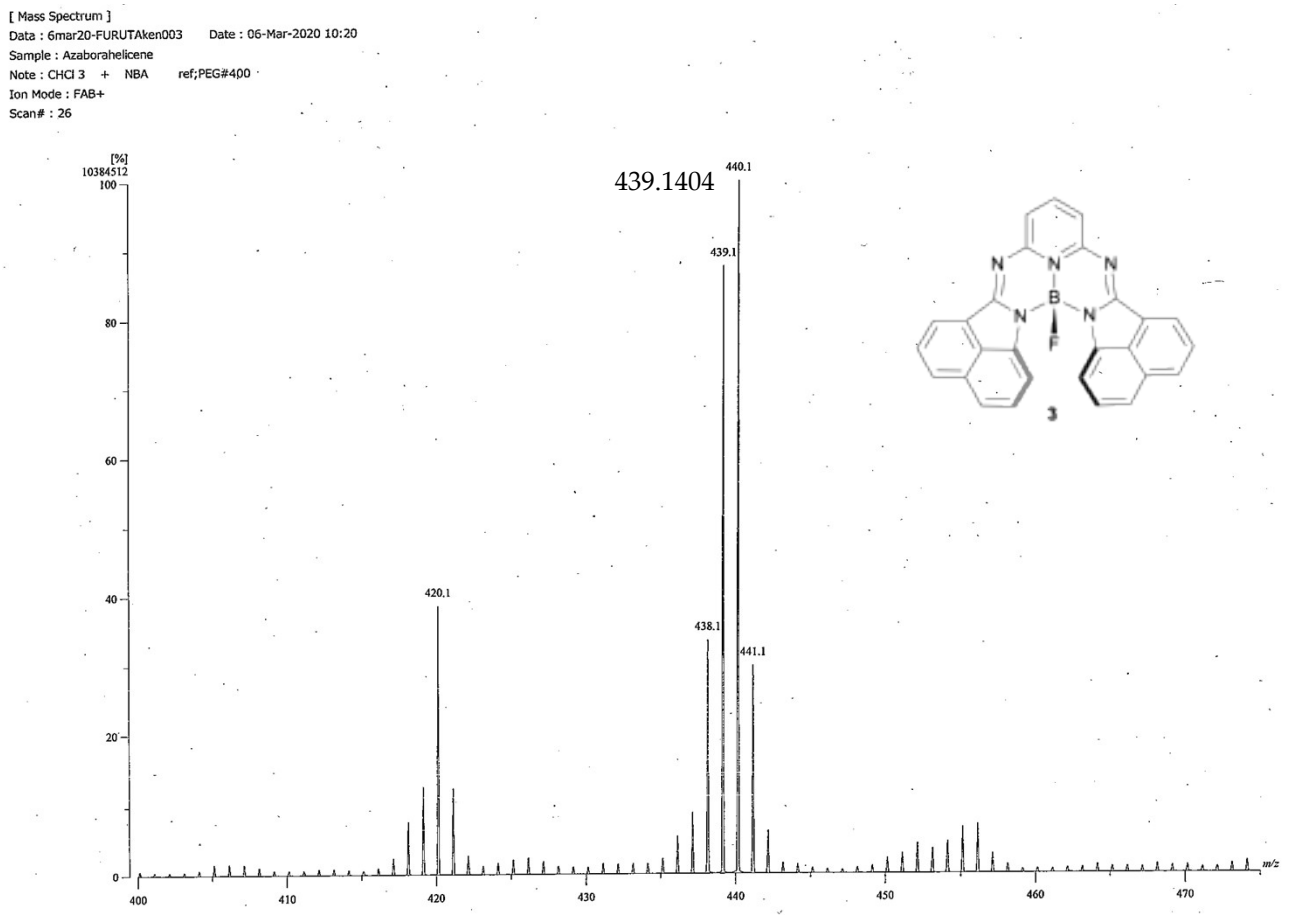

[Theoretical Ion Distribution]
Molecular Formula : C27 H15 B F N5
(m/z 439.1405, MW 439.2590, U.S. 23.0)
Base Peak : 439.1409, Averaged MW : 439.2584(a), 439.2595(w)

m/z	INT.
438.1441	23.0213**********
439.1409	100.0000**********
440.1437	30.6589**********
441.1466	4.6591***
442.1495	0.4587
443.1524	0.0327
444.1553	0.0018

Fig. S1. HR-FAB-MS spectrum of **3** (top) and the isotope pattern (bottom).

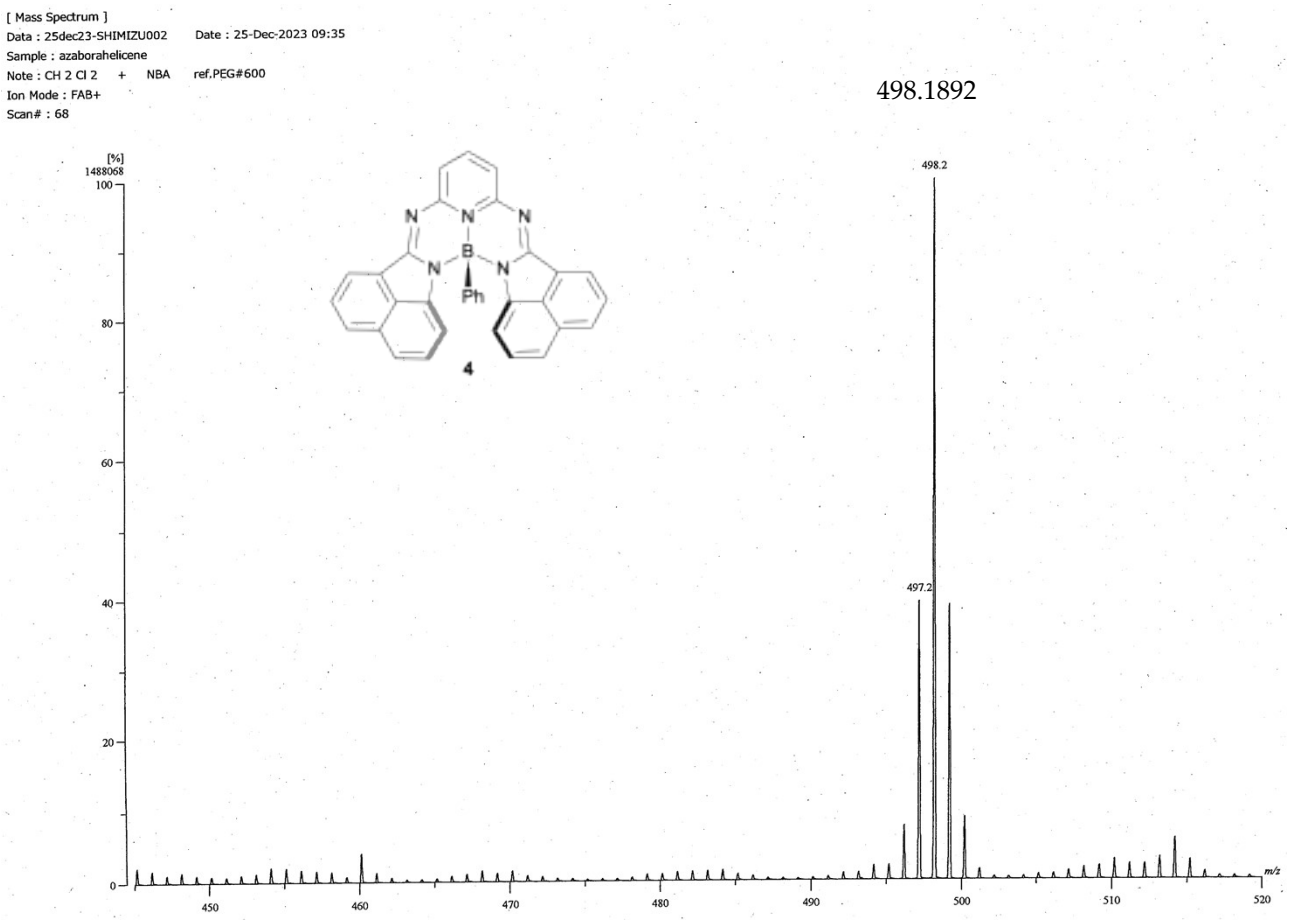

[Theoretical Ion Distribution]
Molecular Formula : C33 H21 B N5
(m/z 498.1890, MW 498.3742, U.S. 26.5)
Base Peak : 498.1896, Averaged MW : 498.3732(a), 498.3743(w)

m/z	INT.
497.1926	22.6730**********
498.1896	100.0000**********
499.1924	36.8095**********
500.1953	6.7870****
501.1983	0.8167
502.2013	0.0718
503.2042	0.0049
504.2072	0.0003

Fig. S2. HR-FAB-MS spectrum of **4** (top) and the isotope pattern (bottom).

iii. NMR Spectra

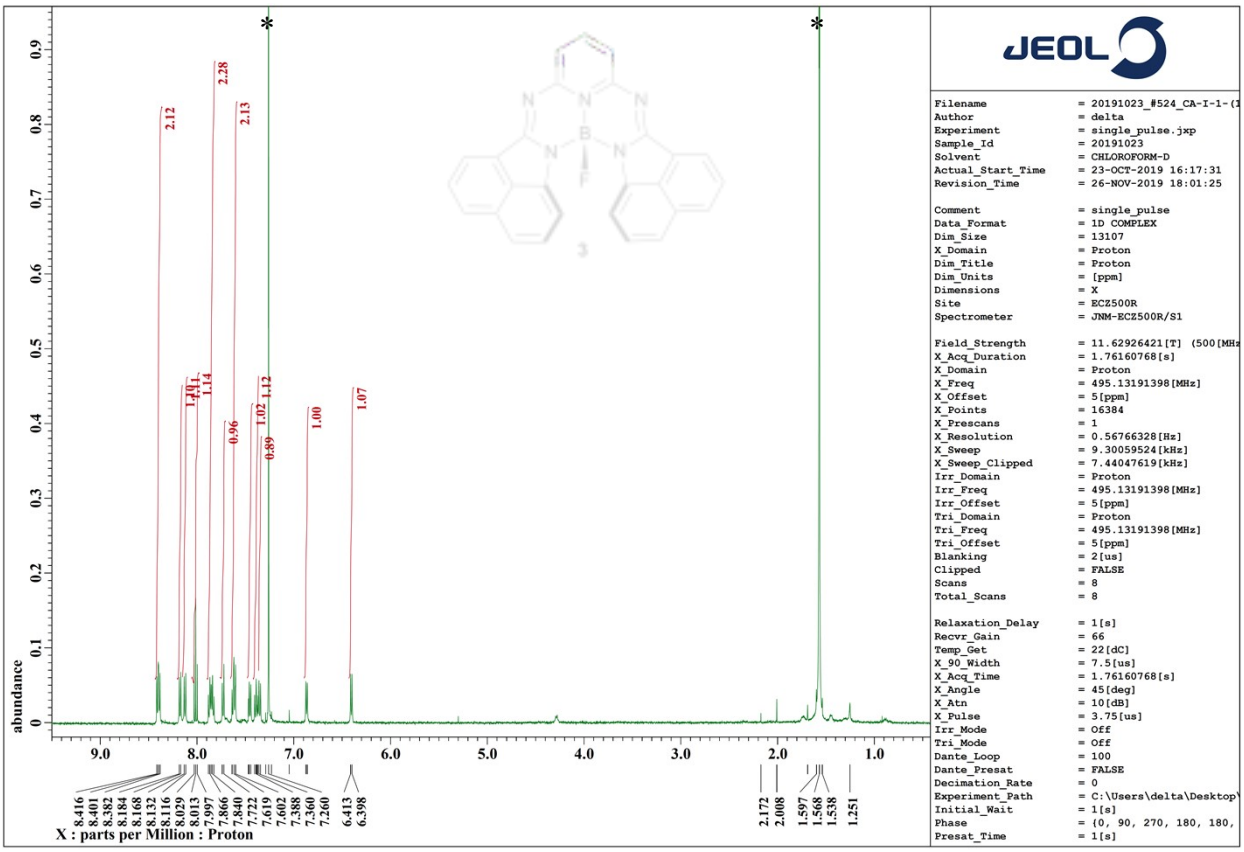

Fig. S3. ^{1}H NMR spectrum of **3** in $CDCl_3$. * indicates a residual solvent signal.

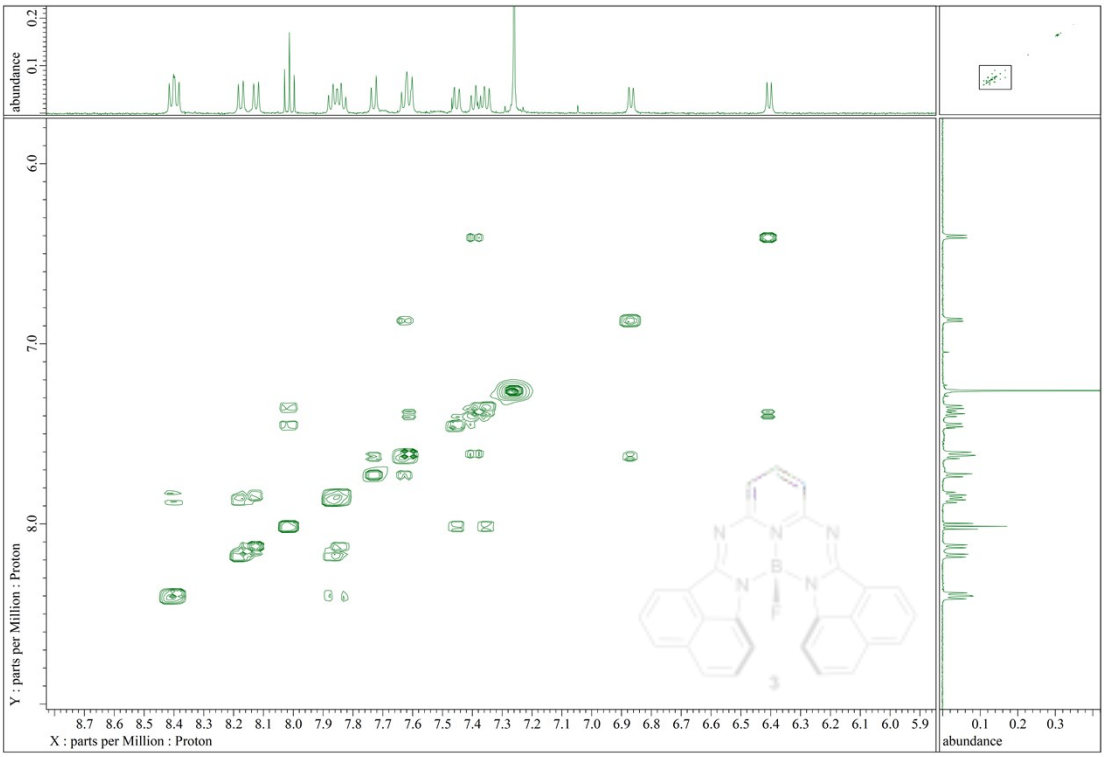

Fig. S4. ^{1}H-^{1}H COSY spectrum of **3** in $CDCl_3$.

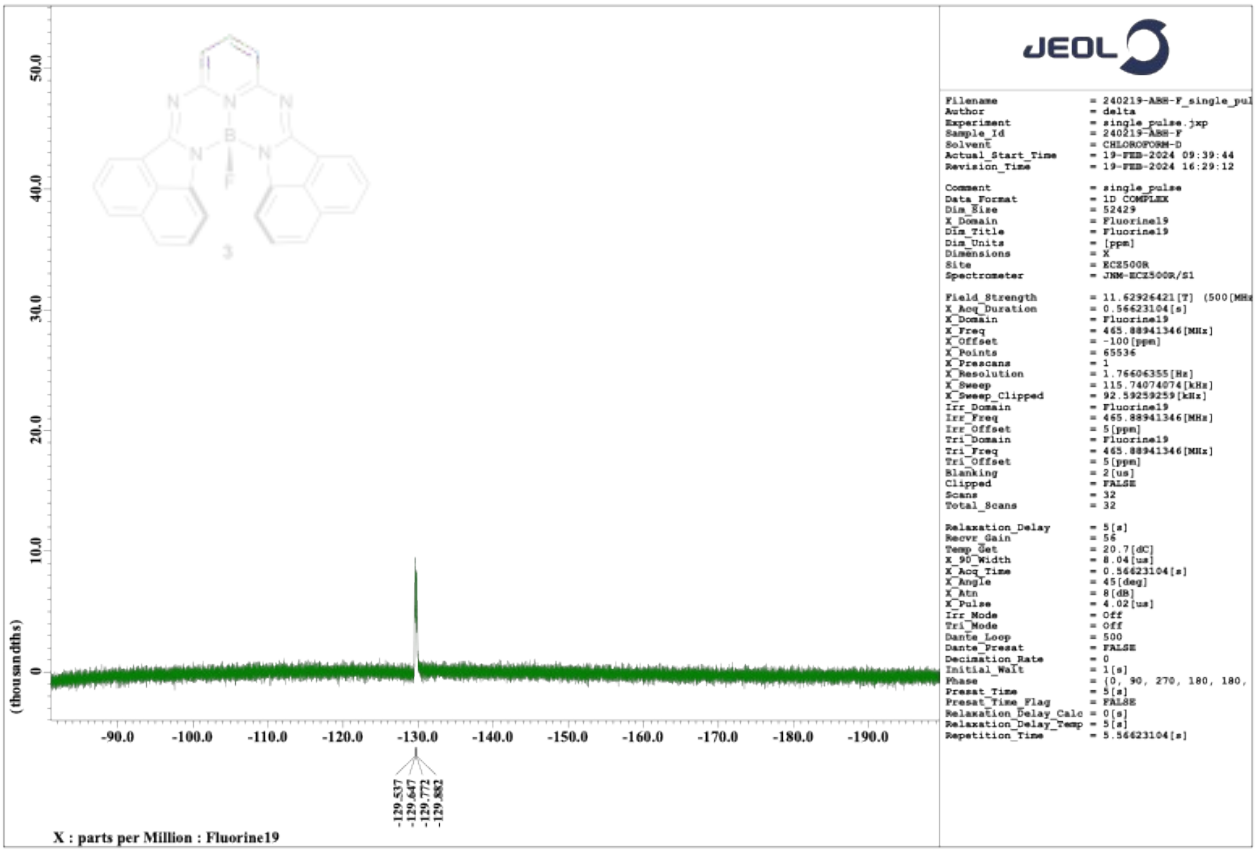

Fig. S5. ^{19}F NMR spectrum of **3** in $CDCl_3$.

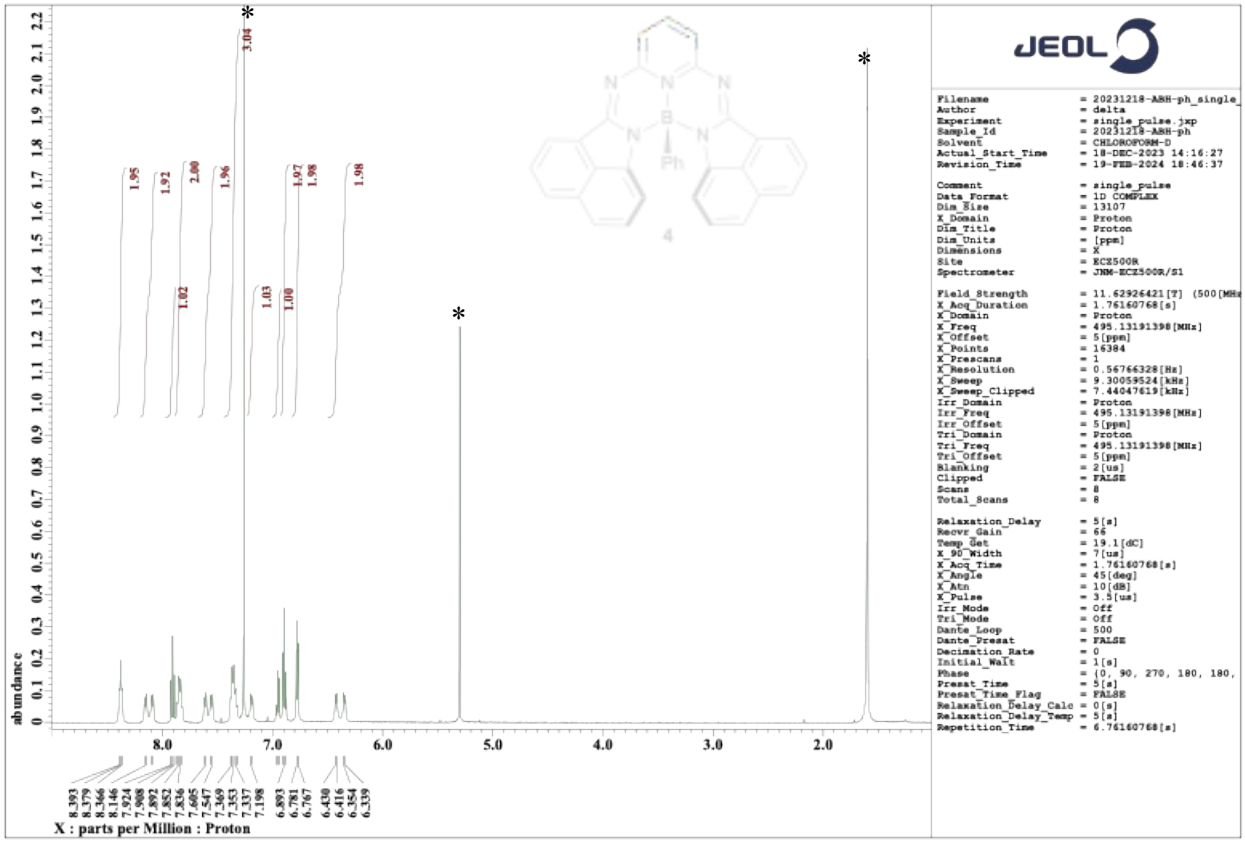

Fig. S6. ^{1}H NMR spectrum of **4** in $CDCl_3$. * indicates residual solvent signals.

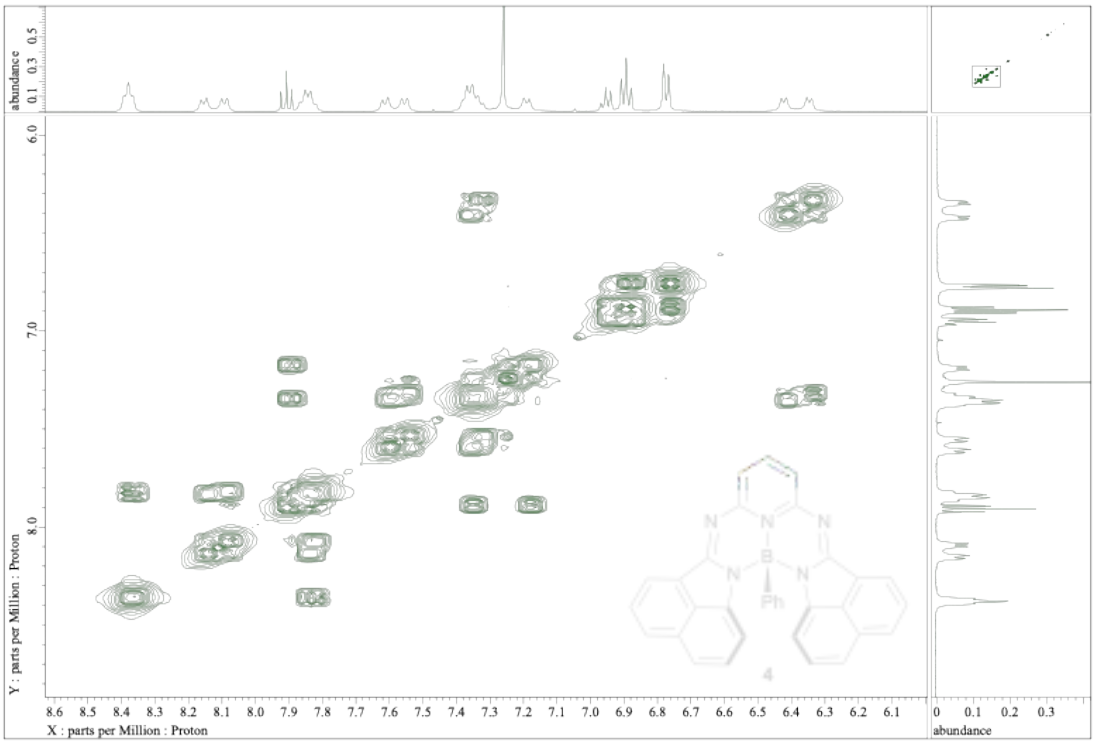

Fig. S7. ^{1}H-^{1}H COSY spectrum of **4** in $CDCl_3$.

iv. Crystallographic Data

Table S1. Crystallographic data.

Compound	**3**	**4**
Empirical formula	$C_{27}H_{15}BF_4N_5$	$C_{34}H_{22}BCl_2N_5$
Formula weight	439.25	582.27
Temperature (K)	100	100
Wavelength (Å)	0.71073 (MoKα)	0.71073 (MoKα)
Crystal system	triclinic	triclinic
Space group	$\bar{P}1$ (no. 2)	$\bar{P}1$ (no. 2)
Unit cell dimensions		
a (Å)	8.0536(5)	9.3419(4)
b (Å)	8.9238(5)	10.0645(5)
c (Å)	15.0934(9)	14.7904(6)
α (°)	79.306(5)	91.141(4)
β (°)	85.035(5)	105.751(4)
γ (°)	65.599(5)	91.019(4)
Volume (Å^3)	970.63(11)	1338.11(11)
Z	2	2
Density (calcd.) (g/cm^3)	1.503	1.445
μ (mm^{-1})	0.098	0.279
F(000)	452	600
Crystal size (mm^3)	0.1 × 0.06 × 0.01	0.24 × 0.18 × 0.02
θ (°) for data collection	2.541 to 27.99	2.024 to 28.28
Index ranges	$-10 \le h \le 10$	$-12 \le h \le 12$
	$-11 \le k \le 11$	$-13 \le k \le 13$
	$-19 \le l \le 19$	$-19 \le l \le 19$
Reflection collected	19008	25738
Unique reflections	4687 (R_{int} = 0.0646)	6621 (R_{int} = 0.0624)
Completeness	1.000	0.994
Absorption correction	multi-scan	multi-scan
Max. and min. transmission	0.779, 1.000	0.770, 1.000
Data/restrains/parameters	4687/0/308	6621/0/379
Goodness-of-fit on F^2	1.039	1.043
Final R indices [I>2σ(I)]	0.0533	0.0562
$wR2$ indices (all data)	0.1286	0.1447
Large diff. peak and hole	0.38, –0.24	0.38, –0.44
CCDC number	2320994	2320995

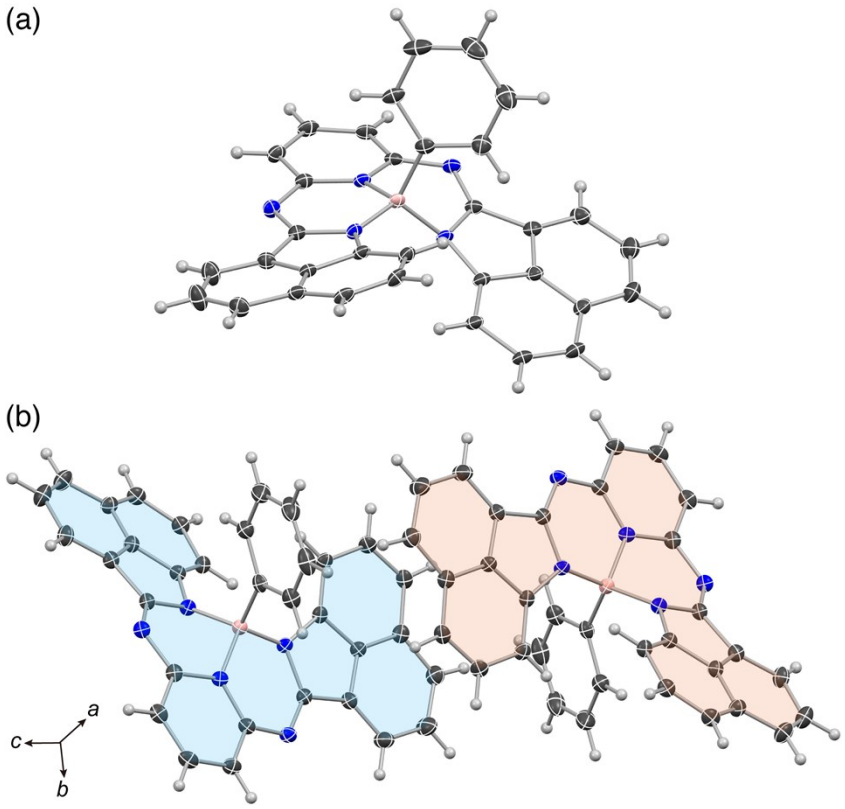

Fig. S8. X-ray single crystal structures of **4**: (a) *P*-enantiomer and (b) packing diagram in which the *P*- and *M*-enantiomers are highlighted in blue and orange colors, respectively. The thermal ellipsoids are scaled to the 50% probability level.

v. Variable-Temperature (VT) ^{1}H NMR Spectra and Simulation

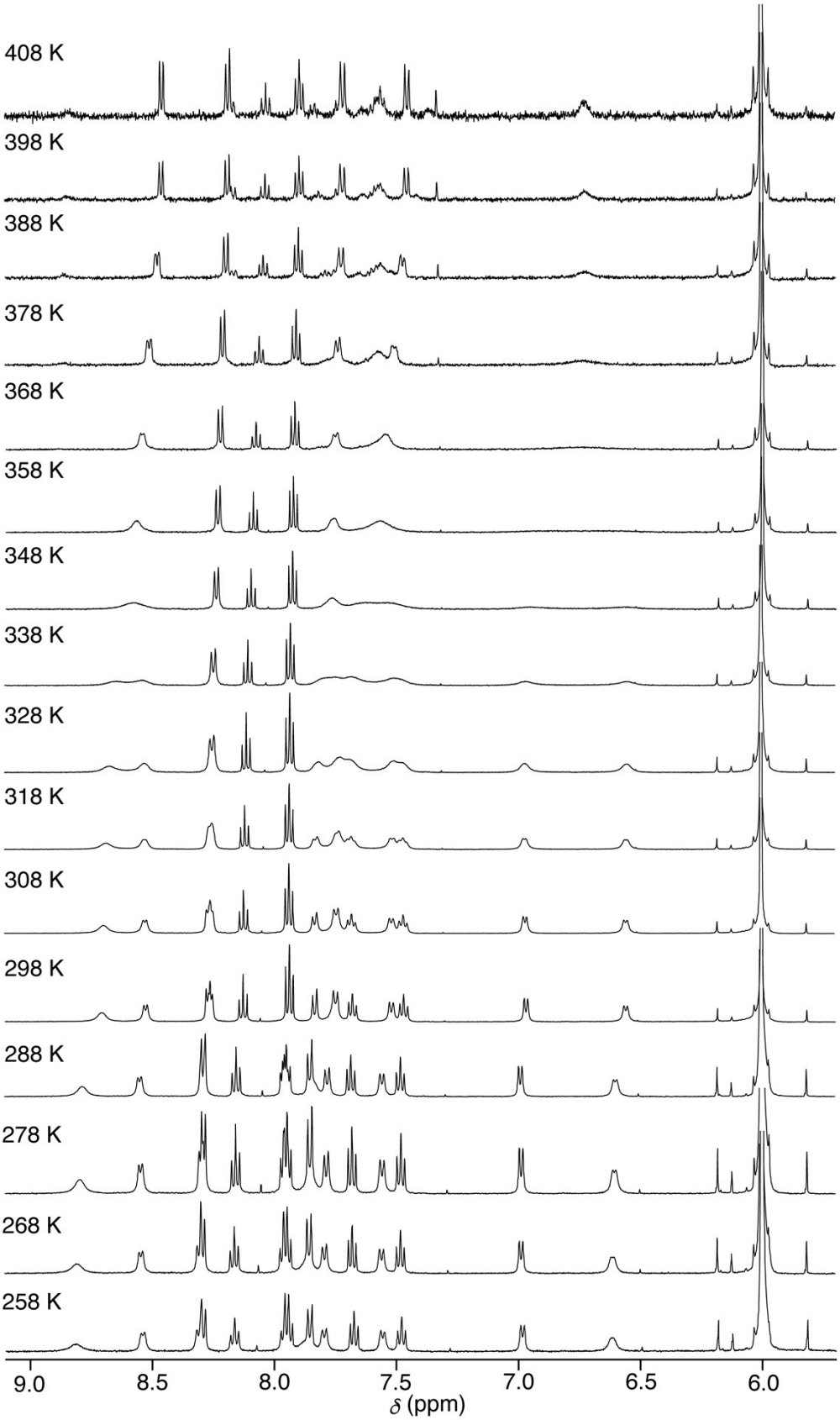

Fig. S9. VT ^{1}H NMR spectra of **3** in 1,1,2,2-tetrachloroethane-d_2.

Line-shape analysis of the proton signals (A, A', B, B', C and C') designated in Fig. S9 was performed using iNMR (ver. 6.4.3).

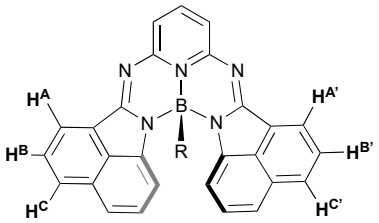

Fig. S10. Protons used for the line-shape analysis in Figs. S11–S14.

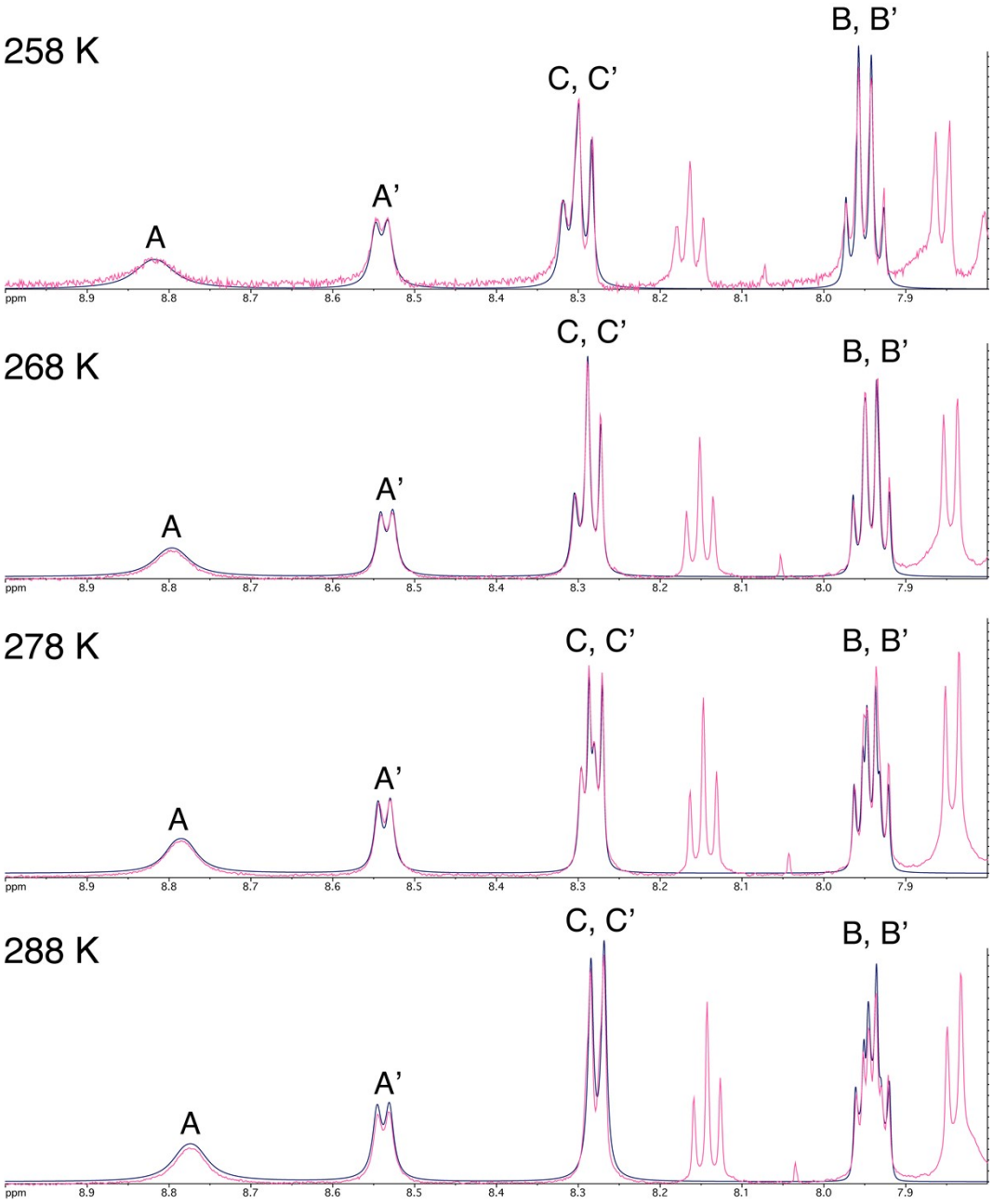

Fig. S11. Observed (pink line) and simulated (blue line) ^{1}H NMR spectra of **3** at 258–288 K in 1,1,2,2-tetrachloroethane-d_2. Inversion rate constants used for the simulation are tabulated in Table S2.

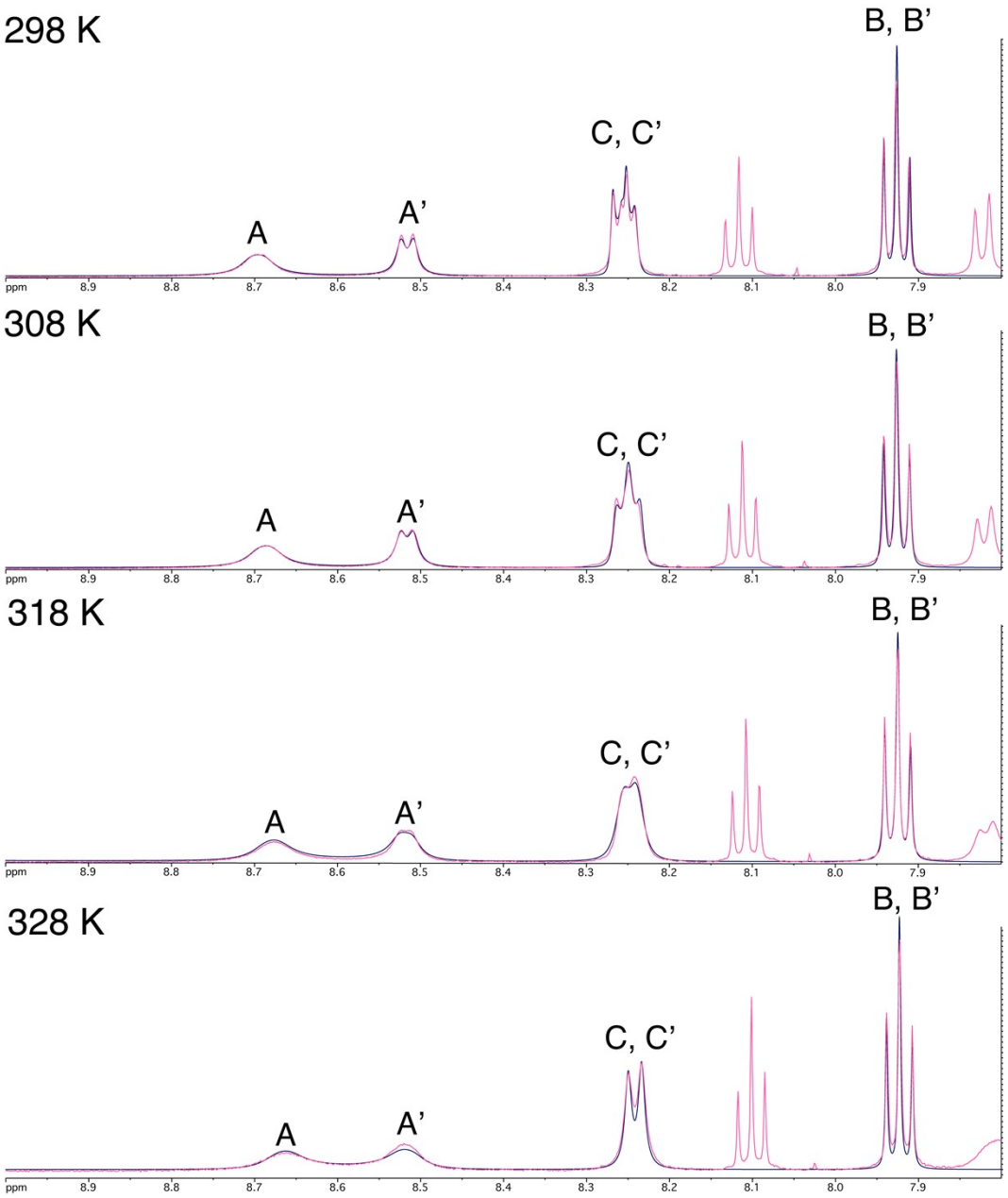

Fig. S12. Observed (pink line) and simulated (blue line) ^{1}H NMR spectra of **3** at 298–328 K in 1,1,2,2-tetrachloroethane-d_2. Inversion rate constants used for the simulation are tabulated in Table S2.

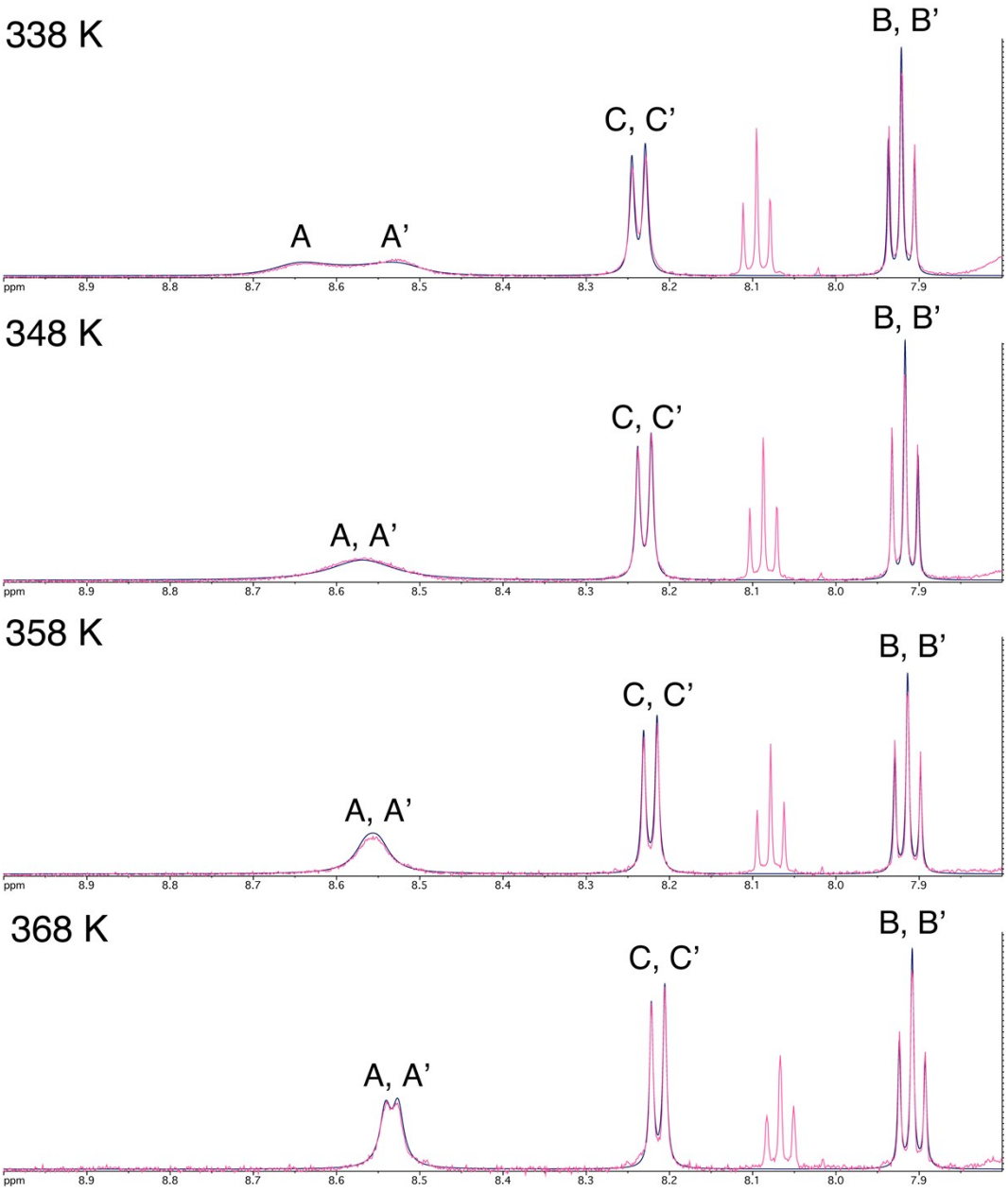

Fig. S13. Observed (pink line) and simulated (blue line) ^{1}H NMR spectra of **3** at 338–368 K in 1,1,2,2-tetrachloroethane-d_2. Inversion rate constants used for the simulation are tabulated in Table S2.

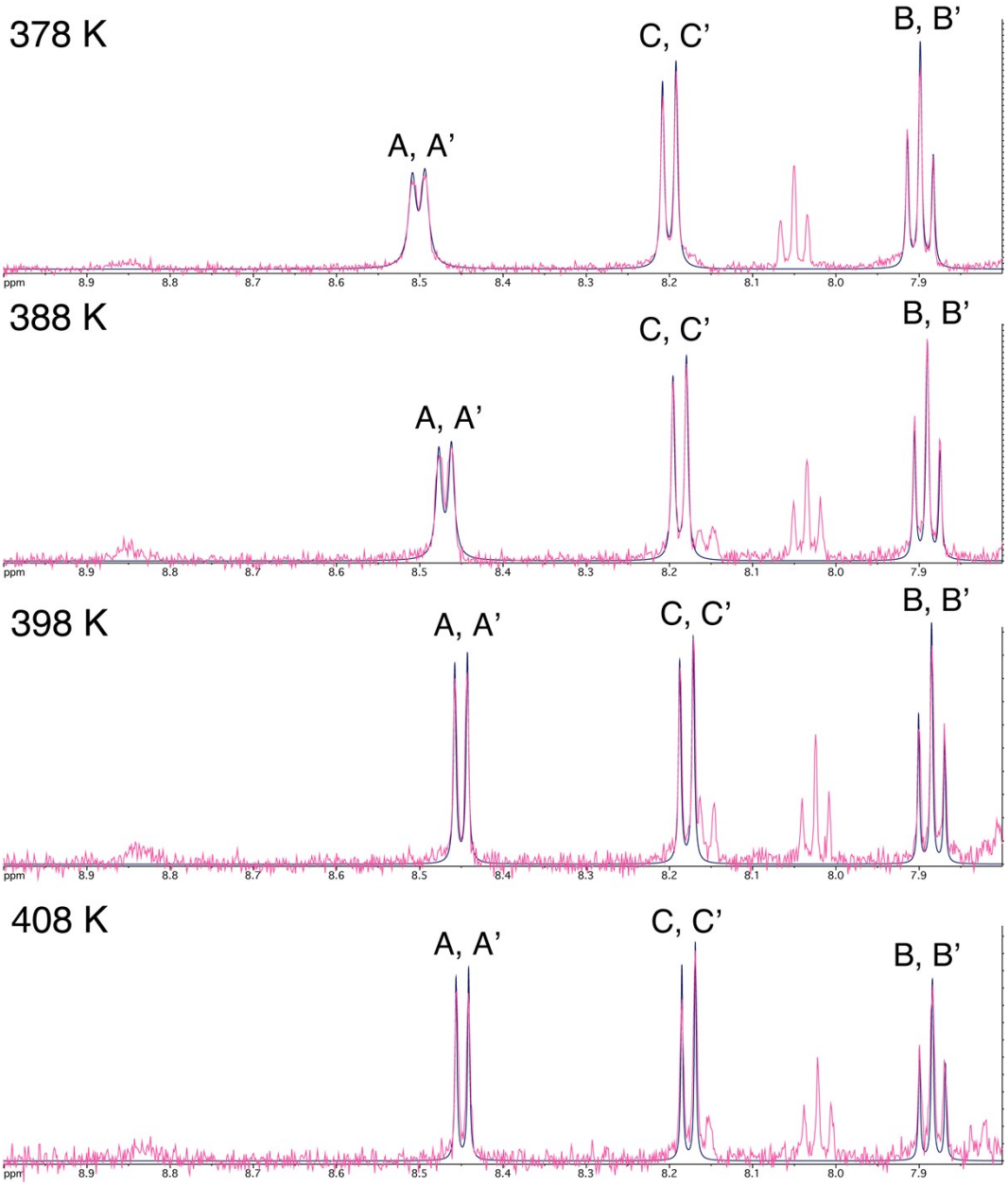

Fig. S14. Observed (pink line) and simulated (blue line) ^{1}H NMR spectra of **3** at 378–408 K in 1,1,2,2-tetrachloroethane-d_2. Inversion rate constants used for the simulation are tabulated in Table S2.

Table S2. Simulated inversion rate constants (k) of **3** at various temperatures.

T [K]	k [s^{-1}]	T [K]	k [s^{-1}]
258	0.2	338	120
268	1.5	348	400
278	2.5	358	600
288	7.0	368	900
298	9.5	378	1200
308	14.5	388	1700
318	40	398	3000
328	60	408	4500

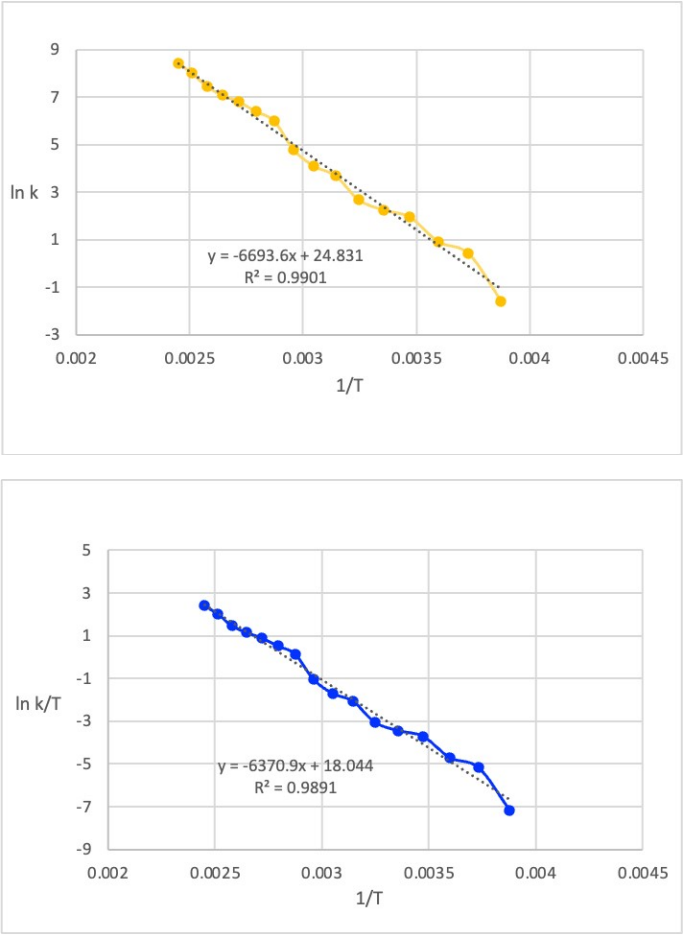

Fig. S15. Arrhenius (top) and Eyring (bottom) plots for **3**.

Table S3. Summary of the activation parameters for **3**.

E_a [kcal mol^{-1}]	13.30±0.35
$\Delta H^{\ddagger}$ [kcal mol^{-1}]	12.66±0.35
$\Delta S^{\ddagger}$ [cal mol^{-1} K^{-1}]	–9.98±1.1
$\Delta G^{\ddagger}_{298}$ [kcal mol^{-1}]	15.70±0.30

vi. Absorption and Fluorescence Spectra of 4

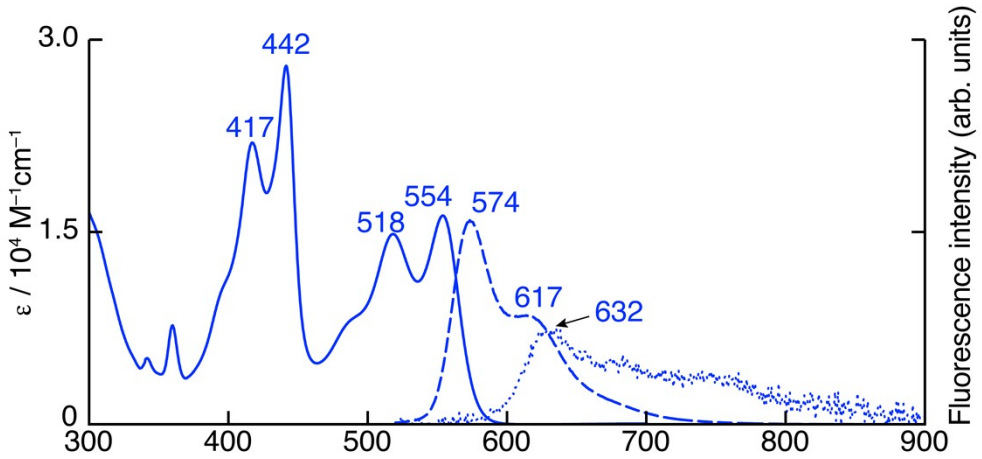

Fig. S16. UV/vis (solid line) and fluorescence (dashed line) spectra of **4** in chloroform and fluorescence spectrum of **4** in a drop-cast film (dotted line).

vii. Electrochemistry of 4

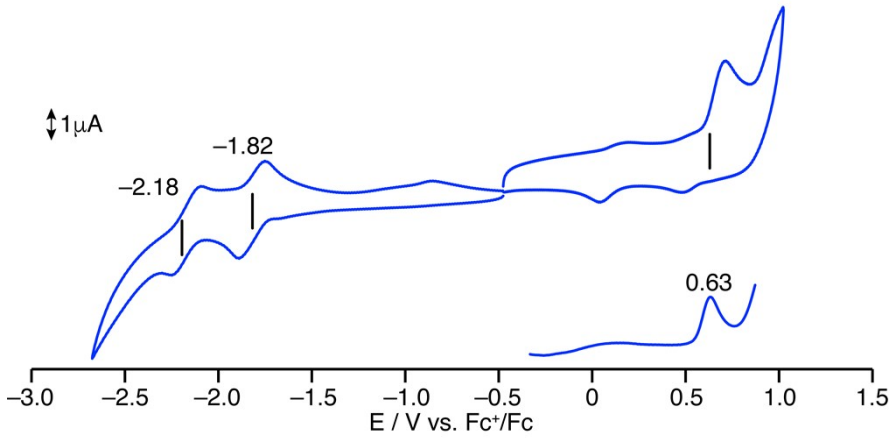

Fig. S17. Cyclic and differential pulse voltammograms of **4** (0.5 mM) in *o*-DCB containing 0.1 M TBAP (scan rare: 100 mV s^{-1} for CV; pulse amplitude: 0.05 V, pulse width: 0.2 s for DPV).

viii. TDDFT Calculations

Table S4. Selected transition energies, oscillator strength and major contributions of **3** calculated by the TDDFT method (B3LYP/6-311G(2d,p). Main contributions are highlighted in bold.

No.	wavelength [nm]	f [a]	Major contributions (weight%)[b]
1	**515**	**0.254**	**HOMO→LUMO (99%)**
2	451	0.067	H–1→LUMO (21%), HOMO→L+1 (77%)
3	**401**	**0.287**	**H–1→LUMO (72%), HOMO→L+1 (18%)**
4	397	0.031	H–1→L+1 (94%)
5	331	0.021	H–4→LUMO (10%), H–3→L+1 (10%), H–2→LUMO (68%)
6	325	0.052	H–3→LUMO (55%), HOMO→L+3 (22%)
7	319	0.012	HOMO→L+2 (83%)
8	309	0.013	H–4→LUMO (23%), H–3→L+1 (15%), H–2→LUMO (21%), HOMO→L+4 (14%)
9	305	0.008	H–7→LUMO (64%), H–6→LUMO (22%)
10	301	0.049	H–3→LUMO (19%), H–2→L+1 (62%)

[a] Oscillator strength. [b] H and L denote the HOMO and LUMO, respectively.

Table S5. Selected transition energies, oscillator strength and major contributions of **5** calculated by the TDDFT method (B3LYP/6-311G(2d,p). Main contributions are highlighted in bold.

No.	wavelength [nm]	f [a]	Major contributions (weight%)[b]
1	**431**	**0.397**	**HOMO→LUMO (96%)**
2	337	0.008	HOMO→L+1 (98%)
3	328	0.088	H–1→LUMO (84%)
4	298	0.031	H–3→LUMO (12%), H–2→LUMO (66%), HOMO→L+2 (16%)
5	294	0.127	H–3→LUMO (61%), H–2→LUMO (18%), HOMO→L+3 (10%)

[a] Oscillator strength. [b] H and L denote the HOMO and LUMO, respectively.

ix. References

1. G. Sheldrick, *Acta. Crystallogr. Sect. A*, 2015, **71**, 3–8.

2. G. Sheldrick, *Acta Crystallographica Section C*, 2015, **71**, 3–8.

3. M. J. Frisch, G. W. Trucks, H. B. Schlegel, G. E. Scuseria, M. A. Robb, J. R. Cheeseman, G. Scalmani, V. Barone, G. A. Petersson, H. Nakatsuji, X. Li, M. Caricato, A. V. Marenich, J. Bloino, B. G. Janesko, R. Gomperts, B. Mennucci, H. P. Hratchian, J. V. Ortiz, A. F. Izmaylov, J. L. Sonnenberg, Williams, F. Ding, F. Lipparini, F. Egidi, J. Goings, B. Peng, A. Petrone, T. Henderson, D. Ranasinghe, V. G. Zakrzewski, J. Gao, N. Rega, G. Zheng, W. Liang, M. Hada, M. Ehara, K. Toyota, R. Fukuda, J. Hasegawa, M. Ishida, T. Nakajima, Y. Honda, O. Kitao, H. Nakai, T. Vreven, K. Throssell, J. A. Montgomery Jr., J. E. Peralta, F. Ogliaro, M. J. Bearpark, J. J. Heyd, E. N. Brothers, K. N. Kudin, V. N. Staroverov, T. A. Keith, R. Kobayashi, J. Normand, K. Raghavachari, A. P. Rendell, J. C. Burant, S. S. Iyengar, J. Tomasi, M. Cossi, J. M. Millam, M. Klene, C. Adamo, R. Cammi, J. W. Ochterski, R. L. Martin, K. Morokuma, O. Farkas, J. B. Foresman and D. J. Fox, *Gaussian 16 Rev. A.03*, (2016), Wallingford, CT.

4. (a) D. Becke, *J. Chem. Phys.,* 1993, **98**, 5648–5652; (b) C. Lee, W. Yang and R. G. Parr, *Phys. Rev. B,* 1988, **37**, 785–789; (c) S. H. Vosko, L. Wilk and M. Nusair, *Can. J. Phys.,* 1980, **58** 1200–1211; (d) P. J. Stephens, F. J. Devlin, C. F. Chabalowski and M. J. Frisch, *J. Phys. Chem.,* 1994, **98**, 11623–11627.

5. B. P. Pritchard, D. Altarawy, B. Didier, T. D. Gibson and T. L. Windus, *J. Chem. Inf. Model.,* 2019, **59**, 4814–4820.

x. Appendix

Table Appx-1. Cartesian coordinates of the DFT optimized geometry of **3** at the ground state calculated at the level of B3LYP/6-311G(2d,p).

Imaginary Freq: 0

Total Energy (Hartree): –1436.9426

	Symbol	X	Y	Z		Symbol	X	Y	Z
1	C	1.431861	4.287492	0.171984	26	C	3.116231	–1.213125	–0.249648
2	C	1.345851	2.899563	0.307399	27	C	–1.540447	–2.055094	1.287495
3	N	0.12755	2.278856	0.142754	28	C	–2.476074	–3.117639	1.447251
4	C	–0.957049	2.968196	–0.339373	29	C	–3.751368	–3.095564	0.927276
5	C	–0.864951	4.348744	–0.522613	30	C	1.035859	–2.268074	–0.767286
6	B	0.035422	0.785325	0.633089	31	C	3.17414	–3.481288	–0.998924
7	N	2.485853	2.183046	0.507692	32	C	1.802008	–3.425382	–1.090068
8	C	2.455388	0.897674	0.282024	33	F	0.131515	0.748129	2.025556
9	N	1.316981	0.14712	0.045128	34	C	0.320597	5.005179	–0.233248
10	N	–2.126563	2.340846	–0.65142	35	H	2.395567	4.746312	0.336588
11	C	–2.260586	1.075202	–0.386415	36	H	–1.742609	4.862348	–0.886148
12	N	–1.31641	0.250441	0.19924	37	H	–6.249104	–2.427341	–0.302376
13	C	–3.500896	0.302658	–0.556294	38	H	–6.701446	–0.294236	–1.401695
14	C	–1.939825	–0.962125	0.557986	39	H	–4.987307	1.500978	–1.551144
15	C	1.709169	–1.156083	–0.321749	40	H	5.42919	1.143153	0.524202
16	C	3.629185	0.02768	0.138313	41	H	6.884869	–0.813765	0.035545
17	C	–3.252442	–0.930173	0.052665	42	H	5.964146	–2.966888	–0.660164
18	C	–4.191394	–1.952578	0.201585	43	H	–2.159298	–3.982965	2.017626
19	C	–5.462331	–1.683714	–0.364534	44	H	1.264068	–4.301704	–1.432577
20	C	–5.716783	–0.470465	–0.985256	45	H	0.387346	6.079397	–0.358586
21	C	–4.748408	0.554388	–1.083216	46	H	3.703341	–4.3886	–1.264949
22	C	4.993053	0.194552	0.237728	47	H	–0.036491	–2.289962	–0.888992
23	C	5.81005	–0.921859	–0.048967	48	H	–0.563469	–2.12088	1.745266
24	C	5.290632	–2.145305	–0.442661	49	H	–4.420194	–3.932745	1.087905
25	C	3.891655	–2.3287	–0.571408					

Table Appx-2. Cartesian coordinates of the DFT optimized geometry of **3** at the transition state for racemization calculated at the level of B3LYP/6-311G(2d,p).

Imaginary Freq: 1

Total Energy (Hartree): −1436.9193

	Symbol	X	Y	Z
1	C	4.336433	0.286143	1.19355
2	C	2.942867	0.19181	1.179591
3	N	2.245514	0.318408	0
4	C	2.942867	0.19181	−1.179591
5	C	4.336433	0.286143	−1.19355
6	B	0.715458	0.813822	0
7	N	2.301894	−0.127549	2.327264
8	C	1.00421	−0.163508	2.340876
9	N	0.133672	0.294373	1.361534
10	N	2.301894	−0.127549	−2.327264
11	C	1.00421	−0.163508	−2.340876
12	N	0.133672	0.294373	−1.361534
13	C	0.238173	−0.621275	−3.501083
14	C	−1.156798	0.353268	−1.965062
15	C	−1.156798	0.353268	1.965062
16	C	0.238173	−0.621275	3.501083
17	C	−1.083042	−0.286718	−3.221885
18	C	−2.135317	−0.43014	−4.131086
19	C	−1.794805	−1.05302	−5.356798
20	C	−0.486139	−1.421476	−5.625329
21	C	0.565305	−1.18827	−4.712907
22	C	0.565305	−1.18827	4.712907
23	C	−0.486139	−1.421476	5.625329
24	C	−1.794805	−1.05302	5.356798
25	C	−2.135317	−0.43014	4.131086
26	C	−1.083042	−0.286718	3.221885
27	C	−2.339029	0.984651	−1.671639
28	C	−3.442834	0.833681	−2.558419
29	C	−3.37961	0.133025	−3.738602
30	C	−2.339029	0.984651	1.671639
31	C	−3.37961	0.133025	3.738602
32	C	−3.442834	0.833681	2.558419
33	F	0.671804	2.20214	0
34	C	5.028516	0.382266	0
35	H	4.827589	0.220893	−2.153124
36	H	−2.56198	−1.220014	−6.104734
37	H	−0.256799	−1.881936	−6.578916
38	H	1.58879	−1.435517	−4.964179
39	H	1.58879	−1.435517	4.964179
40	H	−0.256799	−1.881936	6.578916
41	H	−2.56198	−1.220014	6.104734
42	H	−4.373042	1.316396	−2.282067
43	H	−4.373042	1.316396	2.282067
44	H	−4.248808	0.053228	4.380354
45	H	−2.452499	1.635798	0.827372
46	H	−2.452499	1.635798	−0.827372
47	H	−4.248808	0.053228	−4.380354
48	H	6.109379	0.457877	0
49	H	4.827589	0.220893	2.153124

Table Appx-3. Cartesian coordinates of the DFT optimized geometry of **5** at the ground state calculated at the level of B3LYP/6-311G(2d,p).

Imaginary Freq: 0

Total Energy (Hartree): –1005.0116

	Symbol	X	Y	Z		Symbol	X	Y	Z
1	N	0.354414	2.446274	–0.032261	17	H	–3.51973	–1.396166	0.202984
2	N	–1.609105	1.092016	0.126434	18	H	3.066691	–1.387199	–0.226184
3	C	–0.867801	0.011771	0.080258	19	H	3.155663	–3.863052	–0.293972
4	C	–1.369651	–1.372671	0.079151	20	H	1.150223	–5.256093	–0.200691
5	C	–0.227391	–2.173809	–0.013257	21	C	–1.809037	3.459168	–0.004886
6	C	0.921053	–1.366988	–0.065041	22	H	–2.87814	3.314881	0.058201
7	N	0.49656	–0.026646	–0.000199	23	C	–1.23887	4.698949	–0.133622
8	C	–0.223745	–3.567671	–0.05848	24	C	0.157663	4.815765	–0.224268
9	C	–1.505908	–4.168708	0.003373	25	C	0.909494	3.67338	–0.168099
10	C	–2.647965	–3.387899	0.095887	26	C	–1.003545	2.2994	0.038377
11	C	–2.607158	–1.974672	0.133328	27	H	–1.863182	5.583688	–0.169858
12	C	2.152133	–1.961869	–0.169567	28	H	0.64166	5.775891	–0.332841
13	C	2.186369	–3.385341	–0.213159	29	H	1.988709	3.682437	–0.230853
14	H	–1.598695	–5.248828	–0.02225	30	B	1.369319	1.220895	0.11965
15	H	–3.612746	–3.878926	0.140702	31	F	1.973991	1.317453	1.359315
16	C	1.05912	–4.177104	–0.161054	32	F	2.311001	1.294876	–0.891018